Jestr

Journal of Engineering Science and Technology Review 16 (3) (2023) 52 - 60

Research Article

JOURNAL OF
Engineering Science and Technology Review

www.jestr.org

Performance Analysis of a Two-Stage Converter for Solar PV Systems

Yadlapalli Ravindranath Tagore[1,*], Kandipati Rajani[2] and Alla Ramakoteswara Rao[1]

[1]*Department of EEE, RVR & JC CE, Chowdavaram, Guntur, A.P., India-522019.*
[2]*Department of EEE, VLITS, Vadlamudi, A.P., India-522213.*

Received 1 July 2022; Accepted 30 May 2023

Abstract

The solar based power generation has a significant role all over the world. It has the distinct features like cleanliness and low maintenance costs. However, the solar based power generation is severely affected by the atmospheric solar irradiation fluctuations. Therefore, the maximum power point tracking (MPPT) is necessary in view of enhancing the energy efficiency of the solar PV system. This paper majorly focuses on the solar fed two-stage converter for power system applications. It includes the first stage boost converter (BC) besides the second stage high gain dc-dc converter (HGC). The first stage converter is intended to track peak power from the solar photovoltaic (PV) panel. The P-V as well as I-V characteristics and also MPPT curves of a 230 W solar panel are shown for various solar irradiations. Moreover, this paper highlights the novel beta MPPT algorithm besides the incremental conductance (INC) and perturbation & observation (P&O) algorithms. The beta algorithm has exhibited the dominant dynamics with a transient settling time of 0.1 msec as compared to 0.4 msec and 0.25 msec in case of the INC & P&O MPPT algorithms. The second stage HGC can effectuate the good voltage regulation besides the excellent line and load regulations. The exhaustive simulation results of the voltage mode control (VMC) based HGC are presented in terms of the figure of merits (FOMs) such as transient voltage deviation (TVD) and transient settling time (TST). The VMC is superior with converter dynamics of less than 25 msec as compared to few sec in case of the open-loop operation. The simulation is performed in MATLAB/Simulink as well as PSIM softwares.

Keywords: Solar panel modelling, characteristics, boost converter, peak power point, tracking time, voltage regulation, dynamic performance.

1. Introduction

Over the past few decades, most of the energy utilization is based on the fossil fuels such as natural gas, coal and gas. However, the significant demerits associated with them are the finite resources, environmental emissions and fluctuating costs. In view of this, the renewable energy sources (RESs) such as biofuels, geothermal with fossil fuel power plants, wind and solar are considered as a feasible solution in order to improvise energy growth and reliability. Fig. 1 highlights the latest trends associated with the utilization of the RESs [1]. With the available solar panel funding besides the aggrandizing competitive market prices, the solar energy emanates as the eminent source of energy in many power system applications all over the world. The technology has been predominantly enhanced in the last 20 years at a rapid pace of 20%-25% per year, and has been inverted by solar based battery energy storage systems, engendering solar into a more proficient source of clean energy, as emphasized by Tagore [2]. It has the key advantages like diverse applications, efficiency enhancement of PV modules, advancements in manufacturing technology of power electronic converters, installation at remote locations, reduced dependency on foreign oil and fossil fuels, reduced electricity bills, low maintenance costs, job creation, returns on the investment, cleanliness and technology development. The grid-connected solar PV systems can aggrandize the power capability features of the existed utilities.

On the other hand, stand-alone PV systems are more prominent in feeding power to the distributed loads without the presence of utility. The PV installation systems have a power ranges from few kW to several MW. On the other hand, the down-side is that it highly relies on the weather conditions besides the usage of lot of space. Hence, it is more essential to emphasize the effectual maximum power point tracking (MPPT) controllers in view of obtaining maximum power with respect to the changing weather conditions. The boost converter (BC) is widely used for the solar panel MPPT tracking.

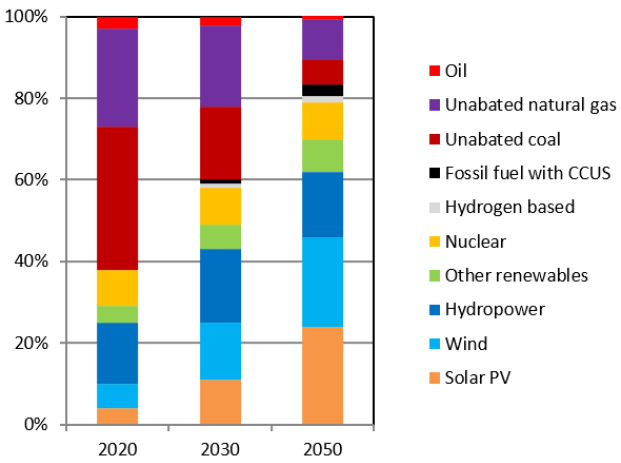

Fig. 1. Future trends of solar enery utilization [1].

*E-mail address: yrtagore@gmail.com
ISSN: 1791-2377
doi:10.25103/jestr.163.07

This paper majorly focuses on the solar fed two-stage converter for the power system applications. The two stage converter proposed by Subbarao et al. [2] consists of a buck and boost converters in the first and second stages. This converter has resulted in high efficiency besides the good output voltage regulation. However, the major disadvantage lies with the poor voltage gain of the second stage converter. It is majorly suited for low voltage applications. A hybrid isolated two-stage BC is proposed by Goyal and Shukla [3]. This has shown to work for a wide range of input voltages. However, the negative effect is the poor voltage conversion ratio of the two stage converter. Another two-stage converter is incorporated with a BC in the first stage and an active switched LC-network associated second stage high gain dc-dc converter (HGC), as emphasized by Tagore et al. [4]. This converter has shown the superior performance with less number of power components and high efficiency. This converter is more preferable for high voltage based power converter applications. However, the down-side is associated with the poor steady state as well as dynamic voltage regulations of the HGC. Therefore, it is important to design a cascade converter that results in high conversion ratio besides the good voltage regulation.

In this research work, the proposed two-stage converter is a cascade connection of the first stage boost converter and the second stage HGC. In the first stage, the foremost MPPT approaches are the Perturb & Observe (P&O) and Incremental-Conductance (INC), presented by Ravindranath et al. [5]. The above algorithms can be predominantly implemented with low memory needs. But, the undesirable performance issues are the inferior accuracy and tracking speed degradation. The choice of perturbation step also affects the converging time and magnitude of oscillations of the MPP. Therefore, this research paper highlights the beta algorithm for the enhancement of the accuracy and tracking speed. Furthermore, the beta algorithm can be perfectly implemented with the microcontrollers, digital signal processing (DSP) and field-programmable gate array (FPGA) controllers. The exhaustive MPPT control approaches and associated simulation results are presented based on the INC, P&O and beta algorithms within the first stage converter. On the other hand, the design of the BC has a significant role in enhancing the lifetime of the photovoltaic module. In view of this, the continuous conduction mode (CCM) operation based BC is preferable that results in the minimization of the sensitivity against the current ripples of the photovoltaic module. The other beneficial aspect is the aggrandized efficiency of the BC. However, this causes a slight rise in the cost of the BC due to 25-30% enlarged size of the inductors and capacitors as contrasted to the discontinuous conduction mode (DCM). The preferable current and voltage ripples for the inductor and capacitor are 15-20 % and 1-3 %.

On the other hand, the CCM based second stage HGC is implemented in order to fulfil the two prominent requirements. The first aspect is boosting the low output voltage from the BC. Otherwise, the purchasing expenditure of photo- voltaic module gets increased in propotion with the higher voltage ratings. The second aspect is associated with the line and load regulations. There exist the various HGCs in the literature designed by Hasanpour et al., Kumar and Veerachary, Yadlapalli et al. [6-10]. The new semiquadratic HGC has resulted in the low input current ripple as well as the reduced device voltage stresses, as designed by Hasanpour et al., [6]. However, it has more number of power components with increased complexity besides the degraded efficiency. Kumar and Veerachary [7] proposed a low cost HGC with the aid of a robust controller. This control strategy can deal the non-minimum phase systems having right half plane zeros. However, the negative effect is the poor voltage gain of the converter. Yadlapalli et al. [8] introduced a HGC for the electric vehicle applications. This converter is implemented with the fuzzy logic control. Moreover, this converter provides high gain besides the good line and load regulations. But the demerit is the poor converter efficiency. Many converter topologies are surveyed by Yadlapalli et al. [9-10]. In many of the above converter topologies, a trade-off is required for the achievable gain and the passive component number. The increased number of power components can curtail the converter efficiency. This research work is based on the switched inductor based HGC for the distributed grid based power system applications. The significant features of this converter are the simplicity, transformer less and reduced stresses, designed by sadaf et al. [11]. As mentioned earlier, there exist the two major issues associated with the line as well as load dynamic regulations of the HGC. In issues related to line regulation, the first stage BC output voltage is not constant and varying. Hence, it is crucial to convert variable output dc voltage of the BC to a fixed voltage by the second stage HGC. On the other hand, the load regulation is important with respect to the voltage dip or rise of the HGC output voltage either for a step increase or decrease of the load or output current. Therefore, the HGC should be implemented with an appropriate closed loop controller in order to provide robustness as well as good dynamic performance against the above mentioned two issues. The controller should provide sufficient bandwidth in view of achieving the fast settlement of the output voltage after following a load disturbance. The achievable phase margin and gain margin should be around 45° and 6 dB. The crossover frequency should be obviously less than the switching frequency. This work focuses on the voltage mode control (VMC) for the HGC and exhaustive simulation results are presented with respect to the large variations in the load changes or the input voltages. The Figure of Merits (FOMs) under consideration are the transient voltage deviation (TVD) and transient settling time (TST). The following are the principal objectives of this research paper:

- To introduce a cost effective and energy efficient multi-stage dc-dc converter for the solar fed power system applications.
- To implement an attractive MPPT algorithm based first stage boost converter in view of achieving better accuracy and tracking speed.
- To design a second stage dc-dc converter with high gain and less number of power components.
- To achieve good converter dynamics with the incorporation of a suitable control strategy in the second stage.

The research paper is configured as given; Section 2 explores the proposed solar PV based power system, and Section 3 presents the modeling aspects along with the MPPT control algorithms. Section 4 highlights the simulation associated with the dynamic analysis of the MPPT controller as well as the HGC based on the VMC. At last, Section 5 presents the conclusions.

2. Proposed Two Stage Converter

The proposed power system contains two-stages as shown in

Fig. 2. As mentioned earlier, the converter in first stage accomplishes the MPP tracking and the second stage converter ensures the line and load regulations.

This work mainly focuses on the modeling aspects of the photovoltaic module. Thereafter, the P-V along with I-V performance characteristic curves are shown with respect to the varying solar irradiations. The response is observed with a step change in the solar irradiations. On the other hand, the second stage converter emphasizes the voltage regulation (VR) aspects of the proposed system. The output dc voltage of the first stage converter is a varying one. Hence, a second stage converter is required to achieve fixed output voltage. Therefore, the loads connected to the second stage converter are not affected by the unregulated output voltage. The exhaustive simulation results are demonstrated for the two stage converter.

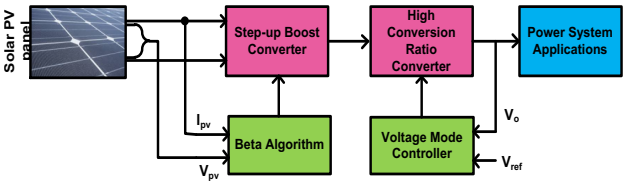

Fig. 2. Solar PV based power system block diagram.

3. Modeling and Dynamic Analysis

3.1. Modeling Aspects

The schematic of HGC is shown in Fig. 3 and the voltage conversion relation given by sadaf et al. [11].

$$\frac{V_{out}}{V_{input}} = \frac{D+1}{1-D} \tag{1}$$

Where V_{out}, V_{in} and D are the dc converter output & input voltages, and duty cycle. Eqs. (2) - (3) present the design aspects of the HGC.

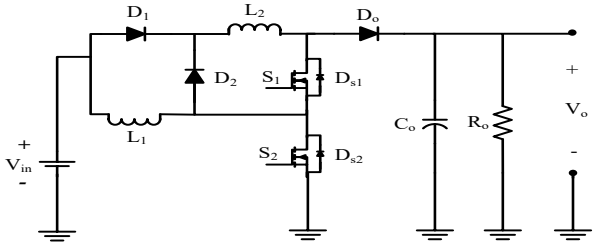

Fig. 3. HGC Schematic diagram.

$$L_1 = L_2 = \frac{V_{in}D}{f_{sw}\Delta i_L} \tag{2}$$

$$C_O = \frac{DP_0}{V_O f_{sw} \Delta V_{CO}} \tag{3}$$

Where L, C_O, P_O, f_{sw}, Δi_L and ΔV_{CO} represent the inductance, output capacitance, output power, switching frequency, inductor current and output capacitor voltage variations or ripples. The dc-dc converter modeling plays a key role in analyzing the dynamics of the converter as given by Yadlapalli et al. [12]. The foremost modeling approach or technique is the state-space averaging. The various control transfer functions are worked out by using Eq. (4).

$$\frac{d\tilde{x_{11}}(t)}{dt} = A_{sss}\tilde{x_{11}}(t) + B_{sss}\tilde{u_{11}}(t) + B_{iii}\tilde{d_{11}}(t)$$

$$\tilde{y_{11}}(t) = C_{sss}\tilde{x_{11}}(t) + E_{sss}\tilde{u_{11}}(t) + E_{iii}\tilde{d_{11}}(t) \tag{4}$$

$$A_{sss} = A_{111s}D + A_{222s}(1-D)$$

$$B_{sss} = B_{111s}D + B_{222s}(1-D)$$

$$C_{sss} = C_{111s}D + C_{222s}(1-D)$$

$$E_{sss} = E_{111s}D + E_{222s}(1-D)$$

$$B_{iii} = (A_{111s} - A_{222s})X + (B_{111s} - B_{222s})U$$

$$E_{iii} = (C_{111s} - C_{222s})X + (E_{111s} - E_{222s})U$$

Where A, B, C, D and E represent the coefficient matrices. $\tilde{x(t)}$, $\tilde{y(t)}$, $\tilde{d(t)}$, $\tilde{u(t)}$ are the small or minute ac fluctuations or perturbations in the state vector, output vector, duty cycle and input vector. Eq. (5) presents the small signal transfer functions.

$$\tilde{x_{11}}(s) = [(SI-A)^{-1}B_{sss} \quad (SI-A)^{-1}B_{iii}]\begin{bmatrix}\tilde{u_{11}}(s)\\ \tilde{d_{11}}(s)\end{bmatrix} \tilde{y_{11}}(s) =$$

$$[C_{sss}(SI-A)^{-1}B_{sss} + E_{sss} \quad C_{sss}(SI-A)^{-1}B_{iii} + E_{iii}]\begin{bmatrix}\tilde{u_{11}}(s)\\ \tilde{d_{11}}(s)\end{bmatrix} \tag{5}$$

The $\frac{\hat{v}o(s)}{\hat{d}(s)}$ transfer function given by Eq. (6) helps to realize the voltage mode control (VMC) strategy.

$$\frac{\tilde{v_o}(s)}{\tilde{d}(s)} = \left(\frac{(v_{output}+v_{input})/(-D+1) - 2I_L SL/(-D+1)^2}{1+2SL/R_O(-D+1)^2 + 2C_O LS^2/(1-D)^2}\right) \tag{6}$$

3.2. Modeling of Solar Cell and Control Algorithm for MPPT

The characteristics of a solar cell resembles like diode characteristics. The single, two and three diode models are widely adopted in the literature, presented by narsipuram et al. [13]. The 2-diode and 3-diode models exhibit good accuracy as differentiated to the 1-diode model. However, the downside is associated with the low computational speed and high complexity. However, the 1-diode models realize a good trade-off between the simplicity and accuracy. Fig. 4 shows the solar or photovoltaic cell model with single diode. The equivalent solar cell mathematical equations are presented by Eqs. (7) - (10).

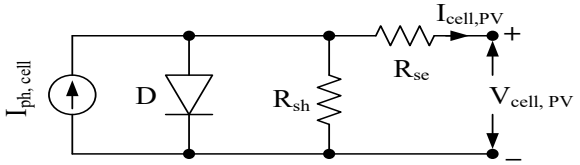

Fig. 4. Solar cell single diode model.

The solar PV cell ($I_{ph,cell}$) photo current is referred by

$$I_{photo,cell} = \frac{G_o}{1000}\left[I_{photo,SO} + (-298 + T_C)K_i\right] \tag{7}$$

The solar PV cell ($I_{cell,PV}$) output current can be indicated as

$$I_{cell,PV} = I_{photo,cell} - I_s\left[exp\left(\frac{(V_{cell,PV}+I_{cell,PV}R_{se})q}{Tka}-1\right)\right] - \frac{V_{cell,PV}+I_{cell,PV}R_{se}}{R_{shunt}} \quad (8)$$

The diode saturation current is notified by

$$I_{saturation} = I_{reversesaturation}\left[\frac{T}{T_{rs}}\right]^3 exp\left[\left\{-\frac{1}{T_{temp}}+\frac{1}{T_{rs}}\right\}\frac{q*E_{gap}}{\text{ak}}\right] \quad (9)$$

Here, the diode reverse saturation current is presented by

$$I_{rs} = I_{satuaration}/\left[exp\left(v_{opencircuit}q/\text{aT}k\right)-1\right] \quad (10)$$

The PV panel ($I_{panelPV}$) output current can be given as

$$I_{solrpanelPV} = I_{photo,panel} - I_{saturation}\left[exp\left(\frac{q(V_{panelPV}+R_{SERIES}I_{panelPV})}{kaTn_s}-1\right)\right] - \frac{I_{panelPV}R_{SERIES}+V_{panelPV}}{R_{SHUNT}} \quad (11)$$

The PV array ($I_{arrayPV}$) output current can be presented as

$$I_{arrayPV} = N_{parallel} * I_{photon,panel} - N_{parallel} * I_s\left[exp\left(\frac{\left(V_{arrayPV}+\left(\frac{N_{parallel}}{N_{series}}\right)I_{arrayPV}R_{SE}\right)q}{Tn_sak}-1\right)\right] - \frac{V_{arrayPV}+\left(\frac{N_{parallel}}{N_{series}}\right)R_{SE}I_{arrayPV}}{\left(\frac{N_{parallel}}{N_{series}}\right)R_{SH}} \quad (12)$$

Where V_{cell}, V_{open}, T, G_O, k, a, q, R_{series}, R_{shunt}, n_s, K_i, N_{series}, $N_{parallel}$ represent the cell voltage, open circuit voltage, temperature (K), solar irradiation (W/m^2), Boltzmann's constant (J/K), ideality factor, electron charge (C), series and shunt resistances (Ω), number of photovoltaic cells, panel temperature coefficent under STC (%/°K). series connected and parallel connected PV modules. MPPT controllers play a key role while grabbing peak solar power. The boost converter is so pertinent in view of fulfilling the above task. Fig. 5 depicts the boost topology.

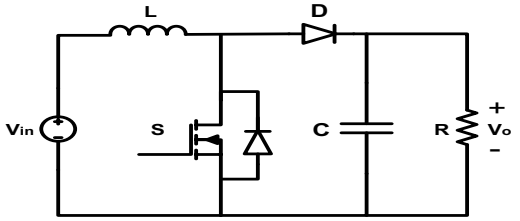

Fig. 5. Boost converter.

3.3. Control Algorithms

3.3.1. INC, P&O and Beta Based MPPT Algorithms

Fig. 6, Fig. 7 & Fig. 8 shows the INC, P&O and beta algorithm based MPPT controllers. In P&O algorithm, the process is involved with the periodical measurement of power and comparing with the previous power. If the solar output power increases, the same step is applied otherwise perturbation is reversed.

These methods fluctuate around the MPP. Therefore, beta algorithm is introduced in order to achieve fast response as well as small oscillations with moderate complexiy. On the otherhand, the Beta method is developed by Jain and Agarwal, Mohammad et al. [14-15]. Eq. (13) presents the intermediate variable β.

$$\beta = ln\left(\frac{i_{panelPV}}{v_{panelPV}}\right) - c \times v_{panelPV} \quad (13)$$

Where $I_{panelPV}$ and $V_{panelPV}$ are the PV module output current and voltages, and diode constant is $c=q/(aN_{series}KT)$. Fig. 8 adresses the Beta based MPPT algorithm. At first, the measurement of current and voltage is fulfilled, so that the β_a value will be repeatedly estimated. If β_a lies in the range of β_{min} to β_{max}, it can be highlighted that the actual operating point is in proximity with the peak power point. Therefore, the Beta approach switches into the stage two, and hence the P&O approach can be implemented in view of enhancing the accuracy as well as curtailing the algorithm complexity. If the β_a is out of this range, then the actual operating point is far away with respect to the peak power point. Then the Beta method shifts to stage one, where, the β_g can be used as guiding value in view of finding the variable step as given below:

$$X_{new} = X_{old} + (\beta_a - \beta_g) * k \quad (14)$$

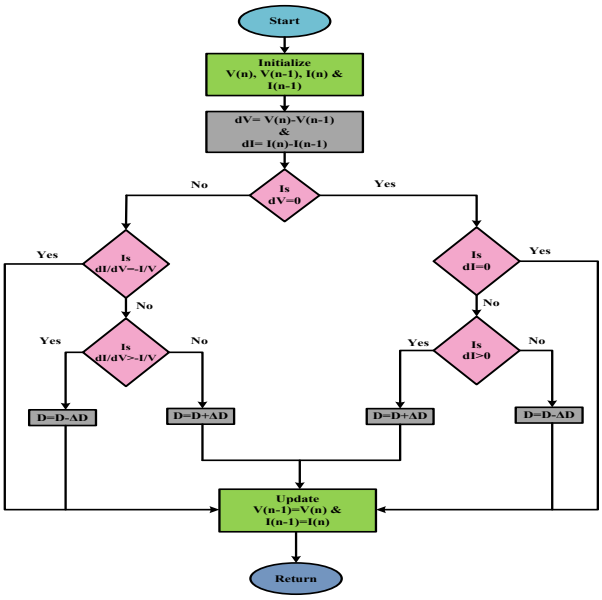

Fig. 6. INC based MPPT algorithm.

Here, X_{old} and X_{new} are the old and new step sizes, the term ($\beta_a - \beta_g$) is the variable step size and k is applied for the regulation of the variable step size. Furthermore, the middle value in-between β_{min} and β_{max} is selected as β_g. Thereafter, the scaling factor k should be optimized in view of effectuating the desired performance.

4. Simulation Parameters and Results

4.1. Solar PV Panel Characteristics

As mentioned earlier, the characteristic curves of a solar panel highly depend on the solar irradiation variations. It results in shifting of the maximum or peak power point of the solar panel. Therefore, it is important to track peak power point and thereby maximum output power will be retrieved from the photovoltaic module. This is called MPPT control technique of the photovoltaic module. Here, the tracking time is more significant with respect to the solar irradiation variations. It can be fulfilled by the BC besides

the development of an efficient MPPT algorithm. At first, the modeling of the solar PV panel is fulfilled in the MATLAB/SIMULINK software. The simulation parameters are taken based on the data sheets of a Tata Power Solar Systems (TP250MBZ) module. The modeling emanates the impact of solar irradiations on the P-V as well as I-V characteristic curves of the photovoltaic module. The output of solar module is connected the first stage BC. The first stage BC will be able to track maximum power point with varying solar irradiations. The BC is simulated by considering the INC, P&O and beta MPPT algorithms individually. The corresponding MPPT curves are shown for different solar irradiation variations. The electrical specifications of a 230 W PV module are shown in Table 1. Where, P_{rated}, V_{peak}, I_{peak}, I_{short} and V_{open} are the rated power, peak voltage, peak current, short circuit current and open circuit voltage of the photo- voltaic module.

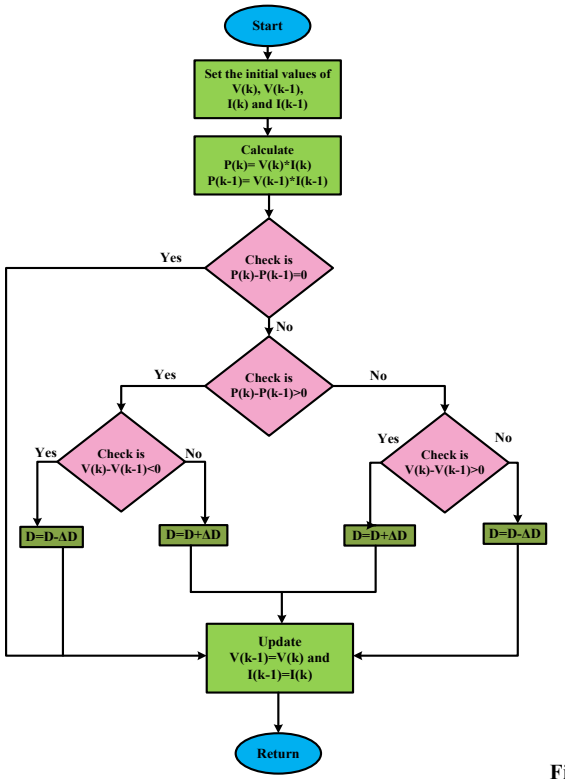

Fig. 7. P&O based MPPT algorithm.

Table 1. Solar panel simulation parameters.

Simulation parameter	Value
Prated	230 W
Vpeak	30 V
Ipeak	9 A
Vopen circuit	37 V
Ishort circuit	9.5 A
Nseries	1
Nparallel	1

Fig. 9(a) highlight the solar panel curves. Fig. 9(b) represents the MPPT curves with solar irradiation variation from higher 1000 W/m^2 to lower 600 W/m^2 and finally step increment to medium 800 W/m^2. Fig. 10 and Fig. 11 present the output voltage of the boost converter and the tracked solar power under steady state. The tracking of solar power is smoother with the beta algorithm, without the presence of any significant oscillations as contrary to the INC & P&O MPPT algorithms. As depicted in Fig. 9(b), the beta algorithm is superior with a tracking time of 0.1 msec tracking time as compared to the 0.4 msec and 0.25 msec in case of INC & P&O based MPPT algorithms.

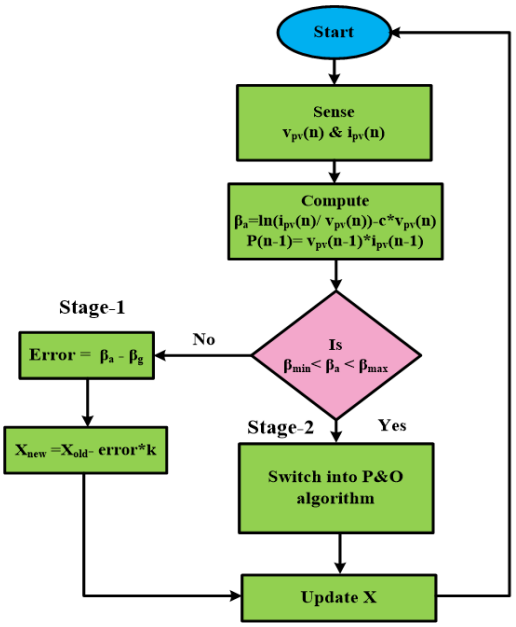

Fig. 8. Beta based MPPT algorithm.

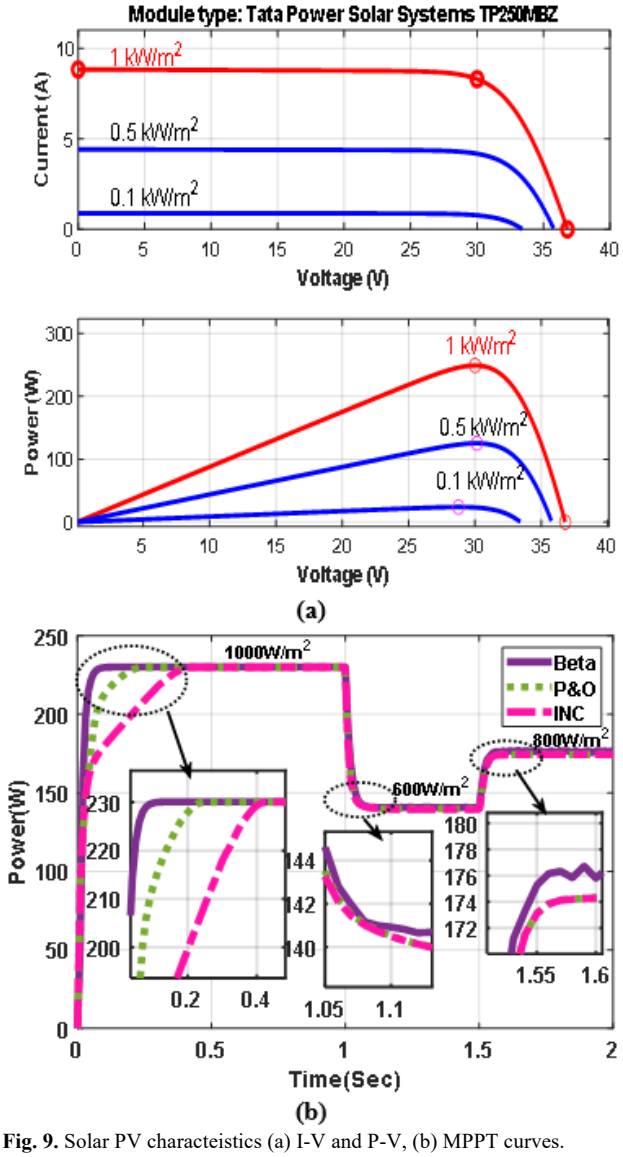

Fig. 9. Solar PV characteistics (a) I-V and P-V, (b) MPPT curves.

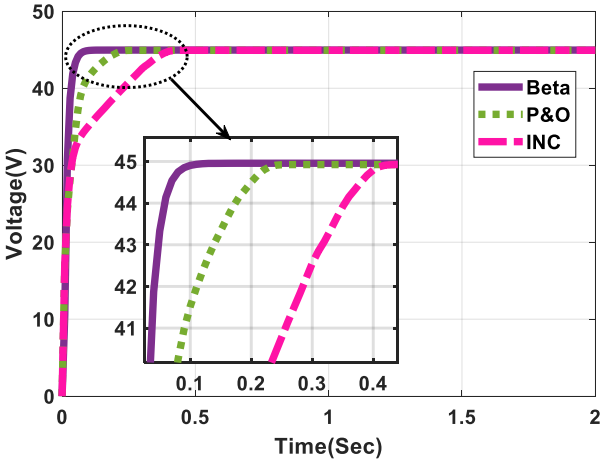

Fig. 10. Output voltage of boost converter.

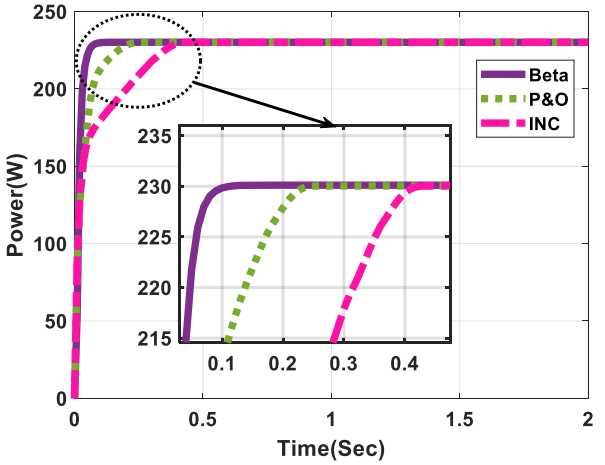

Fig. 11. Tracked solar power under steady state.

4.2 Simulation Study Of HGC

The dc output of the first stage boost converter (BC) is cascaded to the second stage HGC. The second stage HGC is intended to achieve good VR of the output dc voltage. Importantly, the HGC converter is implemented with the voltage mode control (VMC). Fig. 12 emphasizes the block diagram of the VMC based HGC. This control strategy is very simple with one loop. The output dc voltage of HGC is compared with the reference value and the error is fed back to the Propotional Integral (PI) controller. It gives the control signal in order to generate pulse width modulation (PWM) pulses to the switching device.

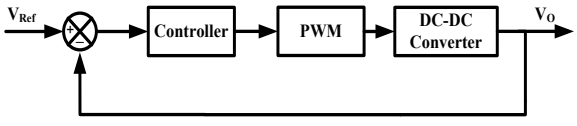

Fig. 12. VMC based HGC block diagram.

The performance of VMC based HGC is justified in terms of the steady state and dynamic voltage regulations (VRs). The steady state VR corresponds to the occurrence of steady state error in the output dc voltage of the HGC. Furthermore, the line and load regulations are associated with the dynamic VR. Either for the line or load regulations, the output dc voltage of the HGC should remain stable and constant. It means that even after the voltage undergoes fall or rise, it should come to steady state within a short period of few msec. The voltage fall or rise is indicated by the performance factor transient voltage deviation (TVD). Whereas transient settling time (TST) corresponds to the time in which the output voltage returns to steady state value after following disturbances such as voltage fall or rise. As per the Institute of Electrical and Electronics Engineers (IEEE) standards, the steady state VR should be less than ±5%, whereas the TVD and TST are around ±15% and 15 msec.

The simulation parameters of the HGC are obtained based on the Eqs. (1) - (3). The control transfer function given by Eq. (6) is helpful while designing the VMC strategy for the HGC. The simulation of the VMC based HGC is fulfilled in PSIM software. The numerous case studies are considered in view of analyzing the dynamic and steady state VRs of the VMC based HGC. Both the MATLAB/SIMULINK and PSIM softwares can be interfaced through PSIM's SimCoupler module. The specifications of the HGC are shown in Table 2. Where V_{in}, L, C_O, R_{max}, R_{min}, K_p and K_i are the input voltage, inductance, output capacitance, maximum and minimum load resistances, PI controller propotional gain and integral gain.

Table 2. Second stage HGC specifications.

Parameter	Value
V_{in}	45 V
L_1	1.436 µH
L_2	1.436 µH
C_o	0.9975 µF
f_{sw}	100 kHz
V_O	400 V
Load R_{min} - R_{max}	1600 - 800 Ω
K_p and K_I	1 & 100

The $\frac{\hat{v}o(s)}{\hat{d}(s)}$ is given by

$$\frac{\tilde{v_o}(s)}{\tilde{d}(s)} = \left(\frac{225-(S35.6e-06}{1+71.8e-06+S^2 71.61e-012}\right) \quad (15)$$

As shown in Fig. 13 (a) and (b), at 45 V input voltage, the steady state output VR of HGC is observed to be 0.5%. As shown in Fig. 14 (a) and (b), at input voltage of 25 V, the steady state output VR of HGC is observed to be 0.5%. On the other hand, as show in Fig. 15, at 45 V input voltage (V_{in}), for periodic load transition from 0.25 A - 0.5 A & 0.5 A - 0.25 A i.e. during the step increment as well as step-decrement load transitions, the TVD and settling times are 12.5%, 11 msec and 12.5%, 22 msec respectively for the VMC based HGC. As shown in Fig. 16, at 25 V V_{in}, for periodic load current transition from 0.25 A - 0.5 A & 0.5 A - 0.25 A i.e. during the step increment as well as step-decrement load transitions, the TVD and settling times are 20%, 20 msec and 12.5%, 7.5 msec respectively. As featured in Fig. 17, during the line regulation study i.e. during the step increase as well as step decrease in input voltage from 45 V - 90 V & 45 V - 25 V the settling times are 40 msec and 25 msec respectively. Fig. 18 shows the input current ripples of 17.1% and 11.25% for different input voltages of 45 V and 25 V.

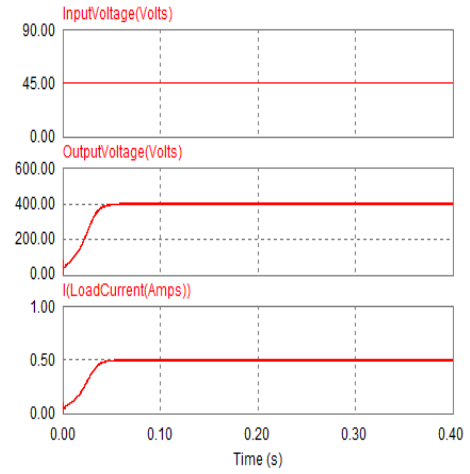

(a)

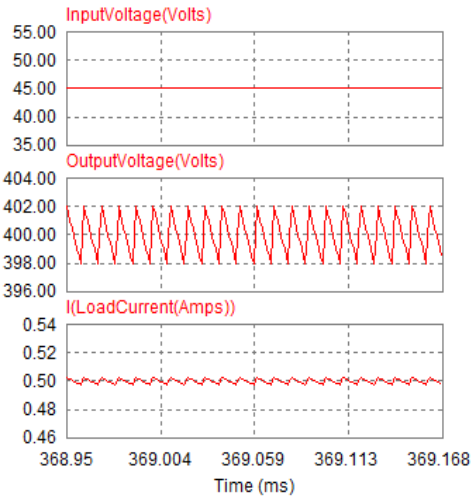

(b)

Fig. 13. HGC waveforms with closed loop control at V_{in}=45 V and load current (I_o) of 0.5 A.

Table 3 to Table 7 enumerate the significant performance outcomes of the proposed two stage converter. As shown in Table 3, the beta MPPT algorithm based boost converter has resulted in a good peak power tracking time of 0.1 msec as compared to 0.4 msec and 0.25 msec in case of the INC and P&O algorithms against the varying solar irradiations. Table 4 highlights the steady state VR of VMC based HGC at different input voltages. The steady state error is found to be less than 1% in both the two cases. These results are seen to be in line with the IEEE standards (5%). Table 5 presents the dynamic load VR of VMC based HGC during the load current variations. The TVDs and TSTs are found to be less than ±20% and 25 msec. Eventhough these values are very little far from the IEEE standards, but still in consideration in case of the non-sensitive loads. For the case of dynamic line VR as shown in Table 6, the worst case scenarios are shown with a large step change in the input voltages. Even in such cases the output dc voltage comes to steady state with settling times of less than 40 msec. As shown in Table 7, the input current ripples shown at different input voltages are acceptable with deviations less than ±20%.

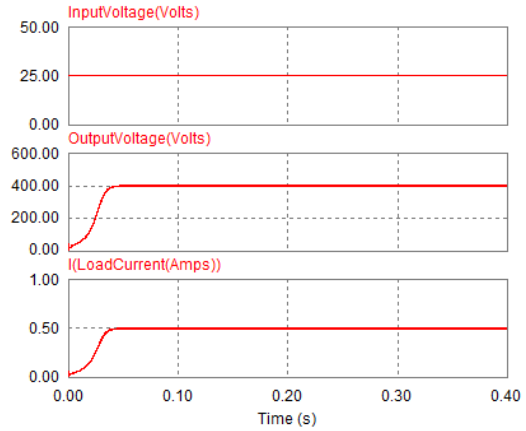

(a)

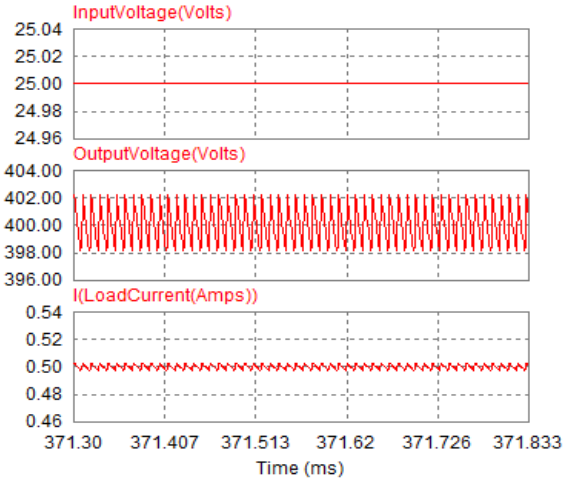

(b)

Fig. 14. HGC waveforms with closed loop control at V_{in}=25 V and load current (I_o) of 0.5 A.

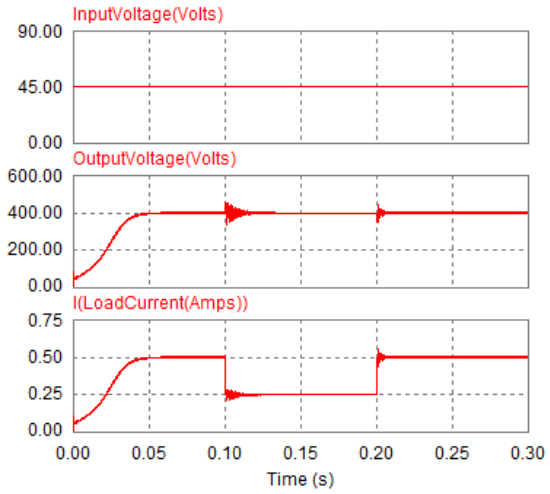

Fig. 15. HGC waveforms with closed loop control at V_{in}=45 V and I_o step from 0.25 A to 0.5 A.

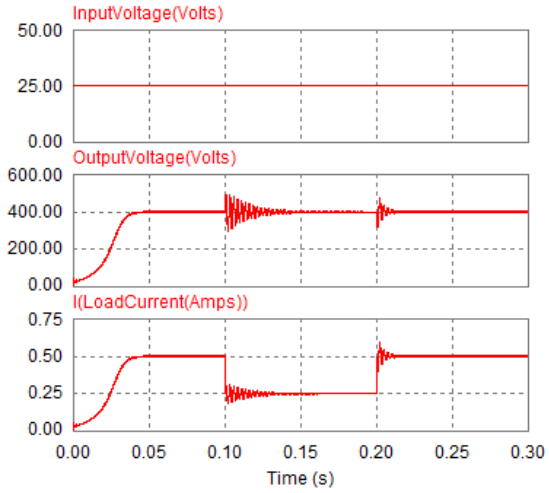

Fig. 16. HGC waveforms with closed loop control at V_{in}=25 V and I_o step from 0.25 A to 0.5 A.

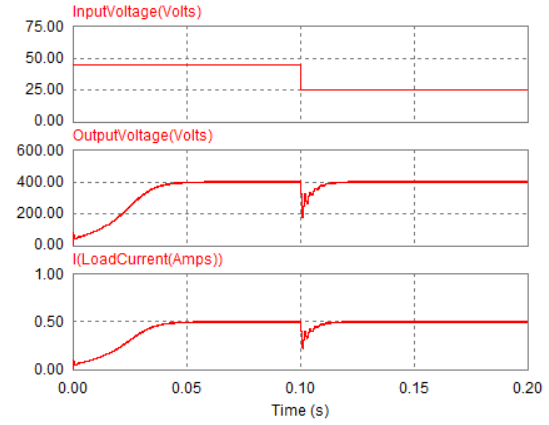

(a)

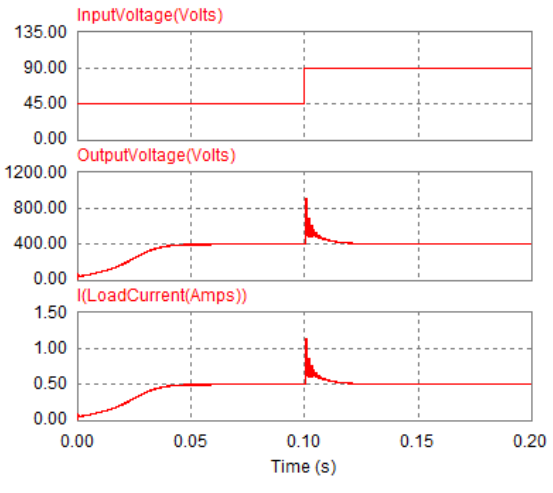

(b)

Fig. 17. HGC waveforms with closed loop control for step V_{in} from (a) 45 V - 25 V & (b) 45 V - 90 V at constant I_o of 0.5 A.

Table 3. Performance comparison of boost converter with different MPPT algorithms.

MPPT Algorithm	Tracking time (msec)
INC	0.4
P&O	0.25
Beta	0.1

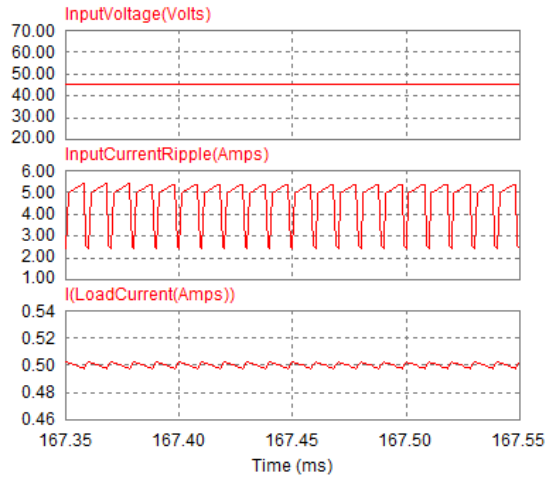

(a)

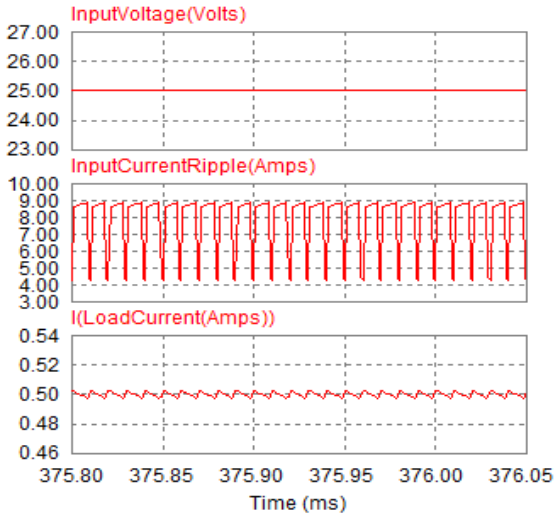

(b)

Fig. 18. Input current ripple at 45 V and 25 V input voltages.

Table 4. Steady state voltage regulation (VR) of VMC based HGC.

	Steady state voltage regulation (VR)	
	At input voltage of 45 V	At input voltage of 25 V
Steady state error (%)	±0.5 %	±0.5 %

Table 5. Dynamic load VR of VMC based HGC.

	Load regulation			
	At input voltage of 45 V		At input voltage of 25 V	
	0.25 A to 0.5 A step load	0.5 A to 0.25 A step load	0.25 A to 0.5 A step load	0.5 A to 0.25 A step load
TVD (%)	-12.5%	+12.5%	-20%	+12.5%
TST (msec)	11	22	20	7.5

Table 6. Dynamic line VR of VMC based HGC.

	Line regulation	
	45 V to 90 V step input voltage	45 V to 25 V step input voltage
TVD (%)	+125%	-45%
TST (msec)	40	25

Table 7. Input current ripple of HGC with VMC.

	At input voltage of 45 V	At input voltage of 25 V
Input current ripple (%)	±17.1 %	±11.25 %

5. Conclusion

This paper explores the modeling and simulation of a multi-stage dc-dc converter fed with the solar power. The imperative aspects are the MPPT control, and converter steady state and dynamic voltage regulations. The MPPT is fulfilled by the first stage boost converter. The solar PV panel characteristics are shown with solar irradiation changing from 100 W/m^2 to 1000 W/m^2. The MPPT controller based on beta approach has exhibited the dominant outcome with a transient settling time of 0.1 msec as contrary to 0.4 msec and 0.25 msec in case of the MPPT algorithms based on INC & P&O. The steady state is also found to be good with beta algorithm. On the other hand, the second stage is the VMC based HGC. The steady state error is found to be less than 1% at different input voltages. This second stage dc-dc converter has exhibited the good load regulation with transient settling times and TVDs of 12.5%, 11 msec and 12.5%, 22 msec during the step increment as well as step-decrement load transitions. At decreased input voltages also the dynamic performance is shown to be good. The HGC also exhibited the good line regulation performance with settling times of 40 msec and 25 msec. The TVDs and TSTs are found to be less than ±20% and 25 msec. The obtained performance indices are in line with the IEEE standards. It is important to have good dynamic performance either in the first stage converter with MPPT or the second stage converter in terms of the load and line regulations. This work can be carried out for high power levels of the two stage converter. The advanced optimizaton or hybrid based MPPT algorithms can achieve the settling times of the order of few usec.

References

1. International Energy Agency, *"Net Zero by 2050:A Roadmap for the Global Energy Sector*" Retrieved from https://www.iea.org/reports/net-zero-by-2050. 2023-01-01/2023-05-20
2. SubbaRao M., Sobhan P. V. S., Sudarsan M. V., and Sai Venkata Ratnam K.. "Design and Implementation of PV Fed Two Stage DC/DC Converter for Home Applications". *Indian Journal of Science and Technology*, 9(S1), 2016, pp.1-6.
3. Goyal V. K., and Shukla A.. "Two-Stage Hybrid Isolated DC-DC Boost Converter for High Power and Wide Input Voltage Range Applications". *IEEE Transactions on Industrial Electronics*, 69(7), 2022, pp. 6751-6763.
4. Ravindranath Tagore Y., Rajani K., and Anuradha K.. "Dynamic analysis of solar powered two-stage dc–dc converter with MPPT and voltage regulation". *Int. J. Dynam.Control*, 10, 2022, pp. 1745-1759.
5. Ravindranath Tagore Y.. "Modeling and Control of Hybrid Power Sourced High Gain DC-DC Converter". *Journal of Engineering Science and Technology Review,* 14 (1), 2021, pp. 119-127.
6. Hasanpour S., Siwakoti Y. P., Mostaan A., and Blaabjerg F.. "New Semiquadratic High Step-Up DC/DC Converter for Renewable Energy Applications". *IEEE Transactions on Power Electronics*, 36(1), 2021, pp. 433-446.
7. Kumar N., and Veerachary M.. "Stability Region Based Robust Controller Design for High-Gain Boost DC–DC Converter". *IEEE Transactions on Industrial Electronics*, 68(3), 2021, pp. 2246-2256.
8. Yadlapalli R. T., Kotapati A., and Srinivasa rao B.. "Fuzzy logic control based high step up converter for electric vehicle applications". *Int. J. Innovative Computing and Applications*. 13(1), 2022, pp. 41-56.
9. Yadlapalli R. T., and Kotapati A.. "Analysis and Design of dc-dc converter for Electric Vehicle Applications". Suranaree J. *Sci. Technol.* 29(4), 2022, pp. 1-10.
10. Yadlapalli R. T., Kotapati A., and Rajani K.. "Advancements in power conditioning units for electric vehicle applications: a review". *International Journal of Electric and Hybrid Vehicles*. 13(1), 2021, pp. 81-115.
11. Sadaf S., Bhaskar M. S., Meraj M., Iqbal A., and Al-Emadi N.. "A Novel Modified Switched Inductor Boost Converter With Reduced Switch Voltage Stress". *IEEE Transactions on Industrial Electronics*, 68(2), 2021, pp. 1275-1289.
12. Yadlapalli R. T., and Kotapati A. "Modeling, Design and Implementation of Quadratic Buck Converter for low power applications." *Int. J. Power Electronics* 11(3), 2020, pp. 322-338.
13. Narasipuram R. P., Chaitanya S., and Yadlapalli R. T.. "Efficiency analysis of maximum power point tracking techniques for photovoltaic systems under variable conditions". *Int. J. Innovative Computing and Applications*, 9(4), 2018, pp. 230-240.
14. Jain S., and Agarwal V. "A new algorithm for rapid tracking of approximate maximum power point in photovoltaic systems." *IEEE Power Electron. Let*t, 2(1), 2004, pp. 16-19.
15. Mohammad Sikander A., Zhang J., Sheng T., and Arshad N. "Modified Beta MPPT Method Based on Actual Climatic Data", In *RCAE 2018: Proceedings of the 2018 International Conference on Robotics, Control and Automation Engineering,* Beijing China Association for Computing Machinery, 2018, pp. 21-29.